Supplementary Material for:

Self-diffusion of water–cyclohexane mixtures in supercritical conditions as studied by NMR and molecular dynamics simulation

Ken Yoshida[1)] and Masaru Nakahara[2)]

[1]*Department of Applied Chemistry, Graduate School of Technology, Industrial and Social Sciences, Tokushima University, 2-1 Minamijyosanjima-cho, Tokushima 770-8506, Japan*

[2]*Institute for Chemical Research, Kyoto University, Uji, Kyoto 611-0011, Japan*

Optimization of the selection of the terms in the polynomial fitting function

The optimization of the selection of the terms in the polynomial fitting function was carried out by minimizing of the average difference between the MD simulation results for the self-diffusion coefficients and the fitted function. The root mean square deviation (RMSD) of the raw MD simulation values ($D_{i,\mathrm{MD}}$) from the fit values $D_{i,\mathrm{fit,MD}}$, $\left[\left(\frac{1}{n_{\mathrm{MD}}}\right)\sum_1^{n_{\mathrm{MD}}}\left(100\left(D_{i,\mathrm{MD}}-D_{i,\mathrm{fit,MD}}\right)/D_{i,\mathrm{fit,MD}}\right)^2\right]^{1/2}$, was calculated for each addition or deletion of a term in the fitting function, and the change was adopted when the addition could decrease the RMSD by more than 0.1% or the deletion did not increase the RMSD by more than 0.1%, so that the optimized form of the polynomial function with the minimum number of necessary terms could be obtained. As an example, let us describe here the final step of the optimization. The optimized function expressed by Eq. (5) in the main text is reproduced here as Eq. (S1):

$$\begin{aligned}\Xi = (1 \quad \phi)\begin{pmatrix} a_{111} & a_{112} & a_{113} & a_{114} \\ a_{121} & a_{122} & a_{123} & a_{124}\end{pmatrix}\begin{pmatrix}1\\ x_{\mathrm{w}}\\ x_{\mathrm{w}}^2\\ x_{\mathrm{w}}^3\end{pmatrix} \\ + \rho(1 \quad \phi)\begin{pmatrix} a_{211} & a_{212} & a_{213} & 0 \\ a_{221} & a_{222} & 0 & 0\end{pmatrix}\begin{pmatrix}1\\ x_{\mathrm{w}}\\ x_{\mathrm{w}}^2\\ x_{\mathrm{w}}^3\end{pmatrix} \\ + \rho^2(1 \quad \phi)\begin{pmatrix} a_{311} & a_{312} & 0 & 0 \\ 0 & 0 & 0 & 0\end{pmatrix}\begin{pmatrix}1\\ x_{\mathrm{w}}\\ x_{\mathrm{w}}^2\\ x_{\mathrm{w}}^3\end{pmatrix}\end{aligned} \tag{S1}$$

The deletion of a term was tested for several of the highest-order included terms, which are shown in red in Eq. (S2):

$$\begin{aligned}\Xi = (1 \quad \phi)\begin{pmatrix} a_{111} & a_{112} & a_{113} & a_{114} \\ a_{121} & a_{122} & a_{123} & a_{124} \end{pmatrix}\begin{pmatrix} 1 \\ x_{\mathrm{w}} \\ x_{\mathrm{w}}^2 \\ x_{\mathrm{w}}^3 \end{pmatrix} \\ + \rho(1 \quad \phi)\begin{pmatrix} a_{211} & a_{212} & a_{213} & 0 \\ a_{221} & a_{222} & 0 & 0 \end{pmatrix}\begin{pmatrix} 1 \\ x_{\mathrm{w}} \\ x_{\mathrm{w}}^2 \\ x_{\mathrm{w}}^3 \end{pmatrix} \\ + \rho^2(1 \quad \phi)\begin{pmatrix} a_{311} & a_{312} & 0 & 0 \\ 0 & 0 & 0 & 0 \end{pmatrix}\begin{pmatrix} 1 \\ x_{\mathrm{w}} \\ x_{\mathrm{w}}^2 \\ x_{\mathrm{w}}^3 \end{pmatrix}.\end{aligned} \tag{S2}$$

The addition of a term was tested for several of the lowest-order omitted terms, which are shown in blue in parentheses in Eq. (S3):

$$\begin{aligned}\Xi = (1 \quad \phi \quad \phi^2)\begin{pmatrix} a_{111} & a_{112} & a_{113} & a_{114} & (a_{115}) \\ a_{121} & a_{122} & a_{123} & a_{124} & 0 \\ (a_{131}) & 0 & 0 & 0 & 0 \end{pmatrix}\begin{pmatrix} 1 \\ x_{\mathrm{w}} \\ x_{\mathrm{w}}^2 \\ x_{\mathrm{w}}^3 \\ x_{\mathrm{w}}^4 \end{pmatrix} \\ + \rho(1 \quad \phi \quad \phi^2)\begin{pmatrix} a_{211} & a_{212} & a_{213} & (a_{214}) & 0 \\ a_{221} & a_{222} & (a_{223}) & 0 & 0 \\ 0 & 0 & 0 & 0 & 0 \end{pmatrix}\begin{pmatrix} 1 \\ x_{\mathrm{w}} \\ x_{\mathrm{w}}^2 \\ x_{\mathrm{w}}^3 \\ x_{\mathrm{w}}^4 \end{pmatrix} \\ + \rho^2(1 \quad \phi \quad \phi^2)\begin{pmatrix} a_{311} & a_{312} & (a_{313}) & 0 & 0 \\ (a_{321}) & 0 & 0 & 0 & 0 \\ 0 & 0 & 0 & 0 & 0 \end{pmatrix}\begin{pmatrix} 1 \\ x_{\mathrm{w}} \\ x_{\mathrm{w}}^2 \\ x_{\mathrm{w}}^3 \\ x_{\mathrm{w}}^4 \end{pmatrix} \\ + \rho^3(1 \quad \phi \quad \phi^2)\begin{pmatrix} (a_{411}) & 0 & 0 & 0 & 0 \\ 0 & 0 & 0 & 0 & 0 \\ 0 & 0 & 0 & 0 & 0 \end{pmatrix}\begin{pmatrix} 1 \\ x_{\mathrm{w}} \\ x_{\mathrm{w}}^2 \\ x_{\mathrm{w}}^3 \\ x_{\mathrm{w}}^4 \end{pmatrix}.\end{aligned} \tag{S3}$$

The RMSD values were examined for both water and cyclohexane. The effect of the changes to Eq. (S1), (S2), or (S3) are summarized in Table SV. It is seen that neither of the changes to Eqs. (S2) or (S3) are acceptable based on the criteria described above, and thus our present conclusion is that the optimized form of the fitting function is the one given by Eq. (S1).

Sources of uncertainties in *D*

The diffusion measurements in this study were performed in the low-density region where the dependence of D on ρ is quite strong (approximately inversely proportional). Instrumentally, the uncertainties in the measurement of D by the pulsed field gradient spin-echo method should be essentially the same between pure and mixture systems, and the uncertainties in the determination of the mole fraction using ^{1}H NMR spectra should be 1−2% at most. The uncertainties along the liquid branch of the coexistence curve, from 30–350 °C and 30–250 °C for water and cyclohexane, respectively, were ±2% on average and ±5% at most for both water and cyclohexane.[1] The density and pressure along the liquid–vapor coexistence curve are uniquely determined by the temperature, and the uncertainty in D herein can be attributed to such factors as temperature fluctuations and inhomogeneity, the magnitude of the field gradient pulses, and the acquisition of the ^{1}H NMR spectra. The uncertainty in the D of one-component systems in the low-density one-phase region, where the density is determined by the chemical shift method, was ±2% on average and ±5% at most.[2] These uncertainties are the same as those along the liquid branch of the coexistence curve, indicating that the uncertainty in the density measurement for one-component systems is smaller than that of the D measurement.

Diffusion in the framework of simple gas kinetic theory

Let us compare the present experimental results extrapolated to extremely low densities using the simplest gas kinetic theory as a reference. This kind of analysis is important not only from the theoretical viewpoint but also from that of applications; for example, the turbine process where multiphase inhomogeneous hot water is involved as a working fluid. It is important to see how the diffusion processes at low densities are controlled by the intermolecular interactions and the microscopic short-range structures given by MD simulation. To this end, the hard-sphere model is very useful for gaining insight into the effect of the attractive interactions; the latter is completely neglected in the hard-sphere model, and thus the deviations of the experimental results from the hard-sphere-model values show us the effect of the attractive interactions. The mutual diffusion coefficient D_{12}^{HS} of a binary mixture of hard spheres is expressed as:[3]

$$D_{12}^{\mathrm{HS}} = \frac{3}{8\pi^{1/2}}\left(\frac{k_{\mathrm{B}}T}{2\mu}\right)^{1/2}\frac{1}{\rho\sigma_{12}^2}, \tag{S4}$$

where μ is the reduced mass, which is related to the masses of hard spheres (m_1 and m_2) by $\frac{1}{\mu} = \frac{1}{m_1} + \frac{1}{m_2}$, k_{B} is the Boltzmann constant, T is the absolute temperature, ρ is the number density of the hard-sphere fluid mixture, and $\sigma_{12} = (\sigma_1 + \sigma_2)/2$, σ_1 and σ_2 being the diameters of the two species. The effect of intermolecular interactions is taken into account by the gas kinetic theory through the collision integral $\langle\Omega\rangle$, which is a function of the intermolecular potential and the temperature. By introducing the collision integral, the mutual diffusion coefficient D_{12} is expressed as:

$$D_{12} = \frac{D_{12}^{\mathrm{HS}}}{\langle\Omega\rangle} = \frac{3}{8\pi^{1/2}}\left(\frac{k_{\mathrm{B}}T}{\mu}\right)^{1/2}\frac{1}{\rho\sigma_{12}^2\langle\Omega\rangle}. \tag{S5}$$

The integral $\langle\Omega\rangle$ has been rigorously obtained for the 6-12 Lennard–Jones (LJ) potential and is tabulated as a function of the scaled temperature $T^* = k_{\mathrm{B}}T/\varepsilon$, where ε is the depth of the potential well.[3] For a binary mixture of different species, ε_{12} for the interaction between different species 1 and 2 in Eq. (S5) can be evaluated from the Lorentz–Berthelot rule, $\varepsilon_{12} = \sqrt{\varepsilon_{11}\cdot\varepsilon_{22}}$, where ε_{11} and ε_{22} are the depths of the potential wells for the interactions between the same species. The mutual diffusion coefficient D_{12} can be estimated from the intra-diffusion coefficients or the self-diffusion coefficients D_1 and D_2, respectively, through the relation expressed:

$$D_{12} = x_1 D_2 + x_2 D_1, \tag{S6}$$

where the activity coefficients are approximated to be unity in the phenomenological context,[4] and this corresponds, in the microscopic context, to the assumption that cross-correlations between the velocities of the two components are the arithmetic means of those for the water–water and cyclohexane–cyclohexane velocity cross-correlations.[5] The experimental quantities determined here are the self-diffusion coefficients of water, D_{w}, and cyclohexane, D_{ch}, in the mixture, and the mutual diffusion coefficient $D_{\mathrm{w-ch}}$ is approximately obtained from Eq. (S6).

The mutual diffusion coefficient $D_{\mathrm{w\text{-}ch}}$ is obtained from Eq. (S6) and is shown in Fig. S11 as a reduced quantity $\rho D_{\mathrm{w-ch}}/\sqrt{T}$ (Eq. (S5)). To gain insight into the experimental results beyond the framework of the simple gas kinetic model for dilute gases, the $\rho D_{\mathrm{w-ch}}/\sqrt{T}$ value obtained experimentally at finite densities was extrapolated to the zero-density limit where use of the simple gas kinetic model is reasonable; the zero-density limit of $\rho D_{\mathrm{w-ch}}/\sqrt{T}$ is denoted here as $(\rho D_{\mathrm{w-ch}})_0/\sqrt{T}$. The $(\rho D_{\mathrm{w-ch}})_0/\sqrt{T}$ value is obtained here practically by employing the average of the $\rho D_{\mathrm{w-ch}}/\sqrt{T}$ values for the lowest density range (ρ = 0.5−1.1 M). This approximation is satisfactory for the present discussion because the dependence of $D_{\mathrm{w-ch}}$ on x_{w} is less at lower values of

ρ, and because the density dependence of $\rho D_{w-ch}/\sqrt{T}$ within the density range from the zero-density limit up to 1.1 M is expected to be within the experimental uncertainty, as shown in Fig. S11. It is to be noted that the MD results shown in Fig. S12 further corroborate the assumption involved in this approximation.

The zero-density-limit values of $(\rho D_{w-ch})_0/\sqrt{T}$ thus determined are plotted as a function of temperature in Fig. S13. The values derived from gas kinetic theory with the hard-sphere and LJ models, as well as the MD simulation results, are all plotted in Fig. S13 for comparison. It is to be noted that the experimental $(\rho D_{w-ch})_0/\sqrt{T}$ values obtained at 250−400 ºC are smaller than those of the hard-sphere model (Eq. (S4)) and the experimental values increase with increasing temperature, indicating the limitations of that model. The attractive interaction between water and cyclohexane plays an effective role even at such high temperatures as 250−400 ºC. The increase in $(\rho D_{w-ch})_0/\sqrt{T}$ with increase in temperature from 250 to 400 ºC is ~10%. This relative increment is similar to that for pure cyclohexane over the same temperature range (~10%)[6] and is much smaller than that for pure water (~30%).[2] A temperature effect of such magnitude on the dynamic interactions between water and cyclohexane is fairly understandable in view of the negligible polarity of cyclohexane; the chemical bonds in cyclohexane are all saturated, in contrast to the unsaturated bonds in the more polarizable benzene molecule. The gas kinetic model with the collision integral for the LJ model (Eq. (S5)) somewhat underestimates the $(\rho D_{w-ch})_0/\sqrt{T}$ values. This can imply that the depth of the potential well $\varepsilon_{w\text{-}ch}$ of the cross-interaction, based on the Lorentz–Berthelot rule, should be an overestimation of the depth of the attractive potential well between water and cyclohexane molecules. A large ε/k_B value of 809 K for a water pair is predominant in the spherical average of the attractive H-bonding interaction between a pair of water molecules, and thus may not be so simply transferable to the pair interactions between water and cyclohexane molecules. The MD results are in excellent agreement with the experimental results in the range 300−400 ºC, the computational approach being much better than the kinetic theory. Such reasonable agreement shows the reliability of the MD method and the pair potentials employed. At temperatures above 500 ºC, the hard-sphere model gives smaller values than the MD results (differences are within 10%). A slight deviation from the hard-sphere model values may be attributed to the use here of the interaction distances σ of the LJ parameter for the hard-sphere diameter, and the σ of the LJ parameter might be an underestimation of the effective repulsive interaction distance, especially in the high-temperature region of 500−800 ºC.

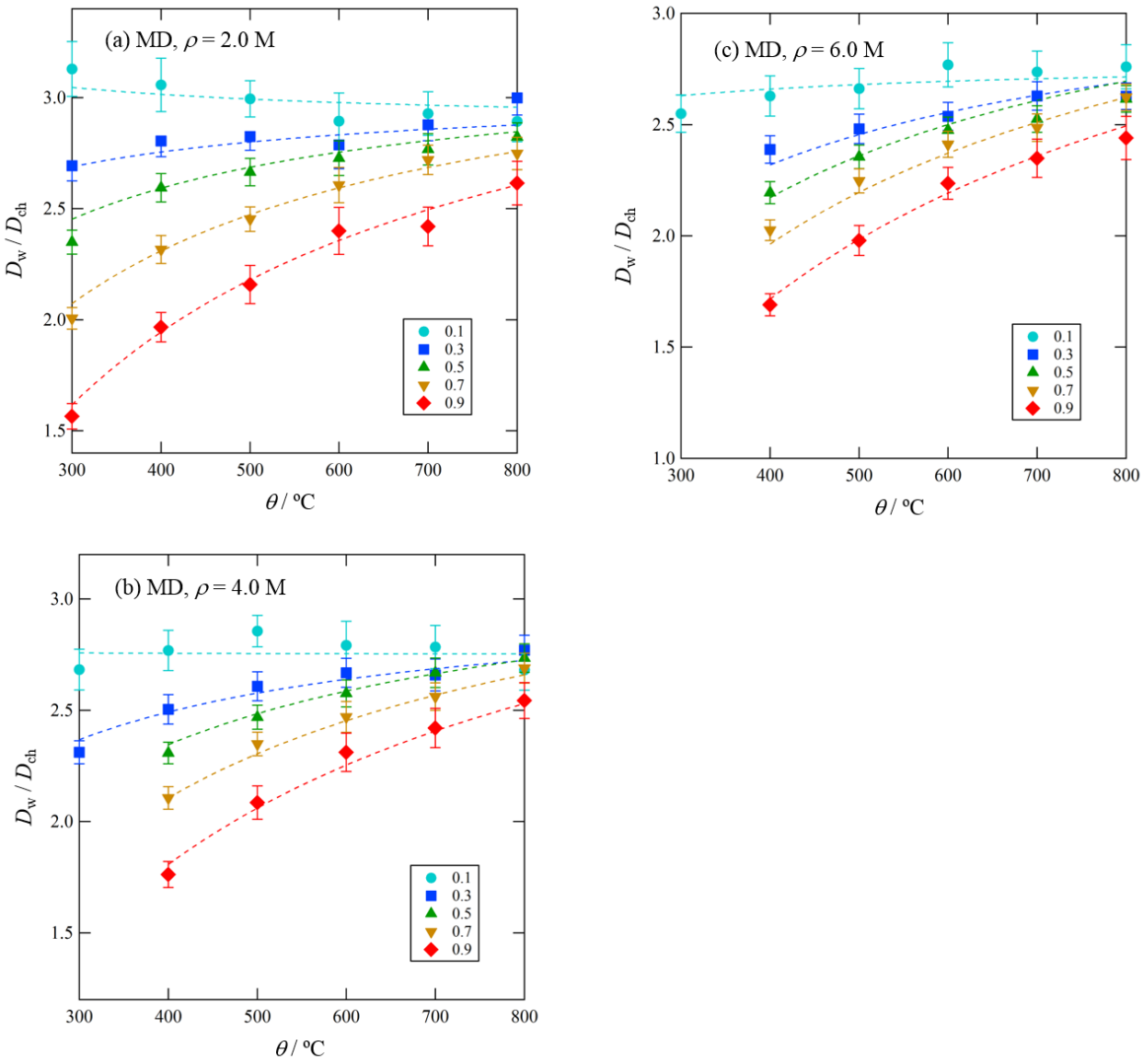

Fig. S1. Ratios of the self-diffusion coefficients of water to those of cyclohexane, D_w/D_{ch}, obtained by MD simulation at (a) 2.0 M, (b) 4.0 M, and (c) 6.0 M. The value for each symbol shown in the figures indicates the water mole fraction x_w. The dashed curves are the fitted values based on Eq. (5).

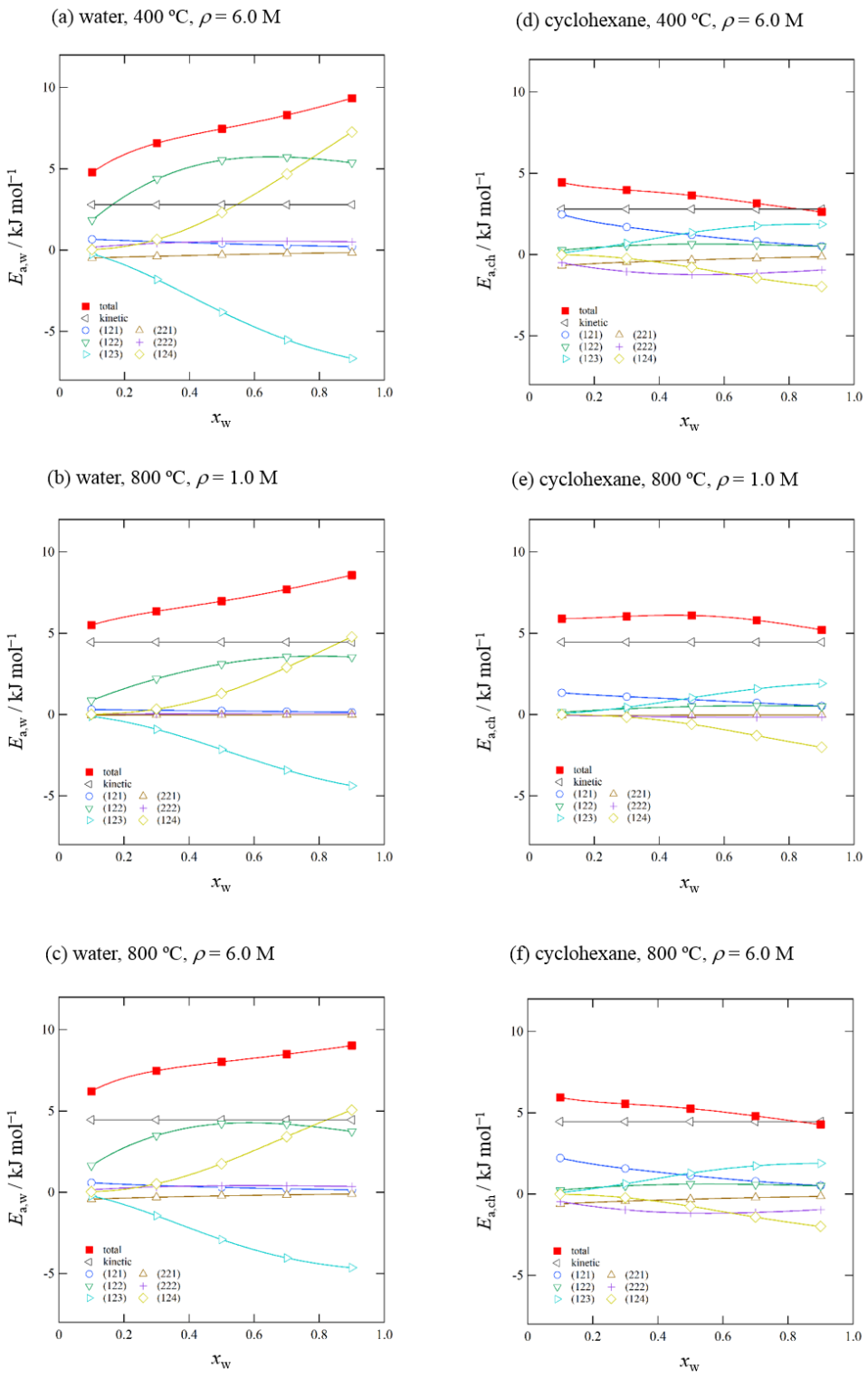

Fig. S2. Overall and component activation energies E_a, $E_{a,kin}$, and $E_{a,klm}$ for the self-diffusion coefficient D of (a) water at 400 °C at 6.0 M, (b) water at 800 °C at 1.0 M, (c) water at 800 °C at 6.0 M, (d) cyclohexane at 400 °C at 6.0 M, (e) cyclohexane at 800 °C at 1.0 M, and (f) cyclohexane at 800 °C at 6.0 M. The relative uncertainty of each term is proportional to that of the associated coefficient listed in Table SIV.

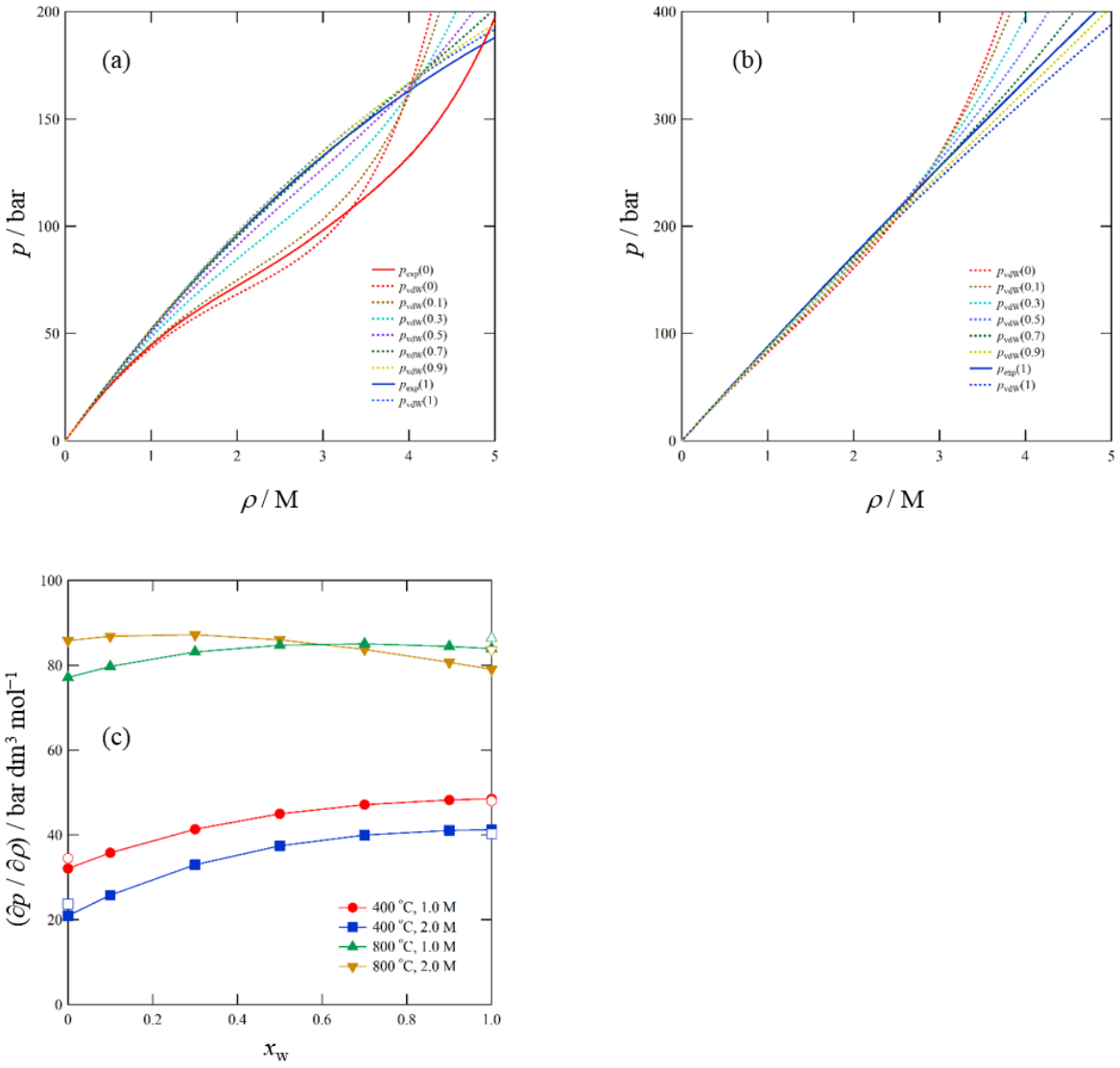

Fig. S3. Pressure of water and cyclohexane calculated by vdW EoS as a function of ρ at (a) 400 °C and (b) 800 °C. (c) The derivative $(\partial p/\partial \rho)$ as a function of x_w at 400 and 800 °C. The open symbols indicate the values for the one-component fluids.

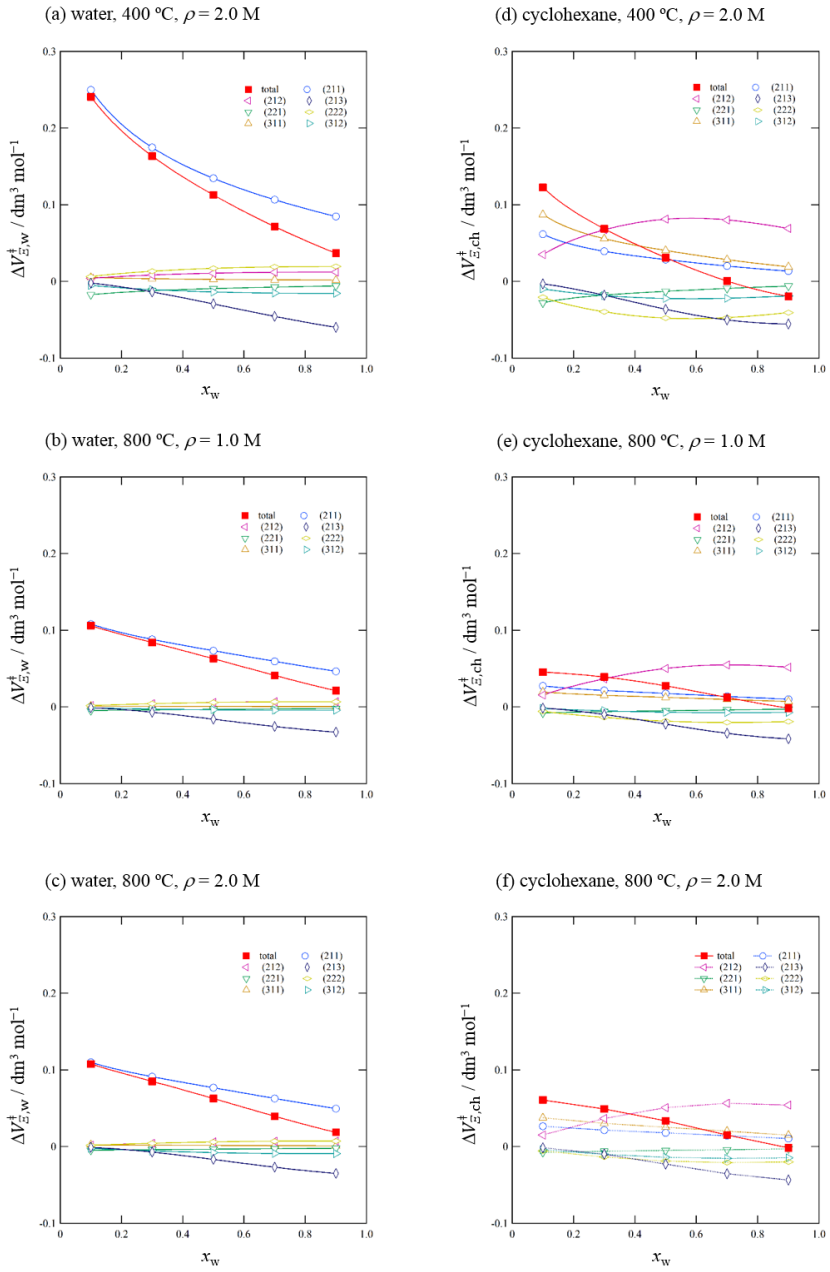

Fig. S4. Scaled and component activation volumes $\Delta V^{\ddagger}_{\Xi}$ and $\Delta V^{\ddagger}_{\Xi,klm}$ of *D* for (a) water at 400 °C at 6.0 M, (b) water at 800 °C at 1.0 M, (c) water at 800 °C at 6.0 M, (d) cyclohexane at 400 °C at 6.0 M, (e) cyclohexane at 800 °C at 1.0 M, and (f) cyclohexane at 800 °C at 6.0 M. The three-digit number for each plot indicates the subscript *klm* of $\Delta V^{\ddagger}_{\Xi,klm}$. The relative uncertainty of each term is proportional to that of the associated coefficient listed in Table SIV.

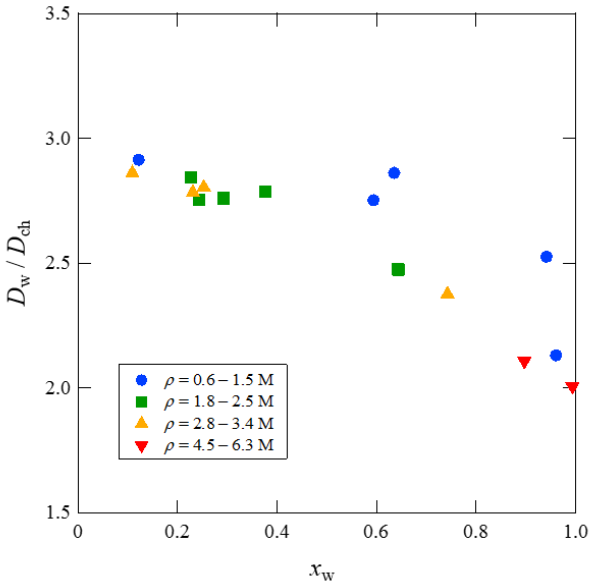

Fig. S5. Ratio of the self-diffusion coefficient of water to that of cyclohexane, D_w/D_{ch}, obtained from NMR experiments at 400 ºC, plotted against the water mole fraction x_w.

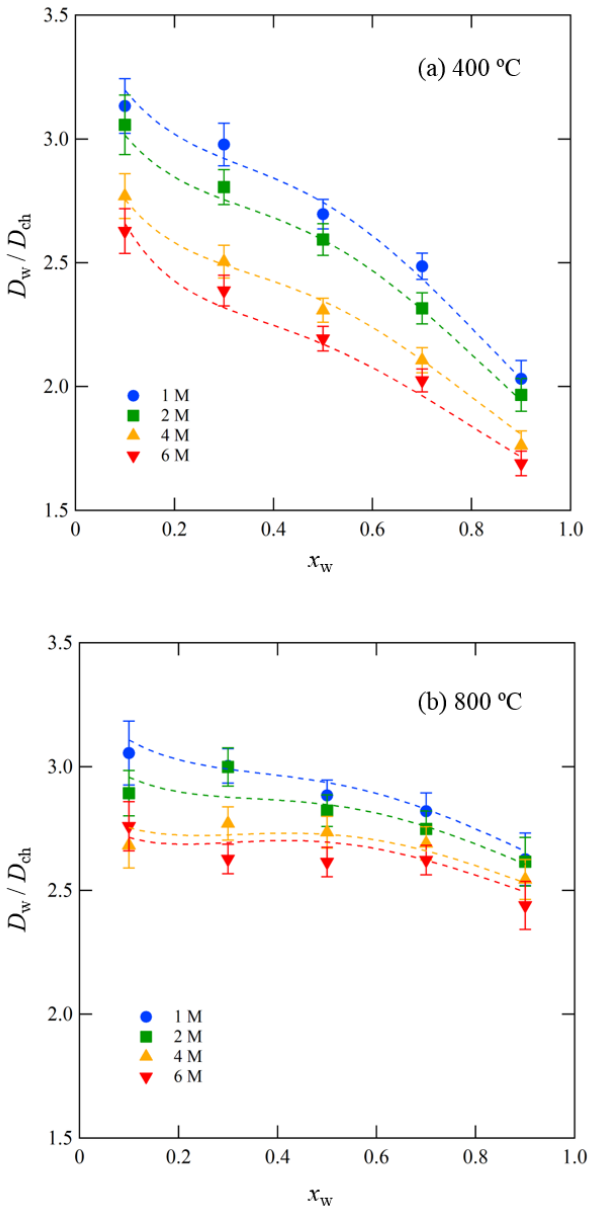

Fig. S6. Ratio of the self-diffusion coefficient of water to that of cyclohexane, D_w/D_{ch}, obtained by MD simulation (a) at 400 ºC and (b) at 800 ºC plotted against the water mole fraction x_w. The dashed curves are the fitted values based on Eq. (5).

(a) 400 ºC, ρ = 2.0 M

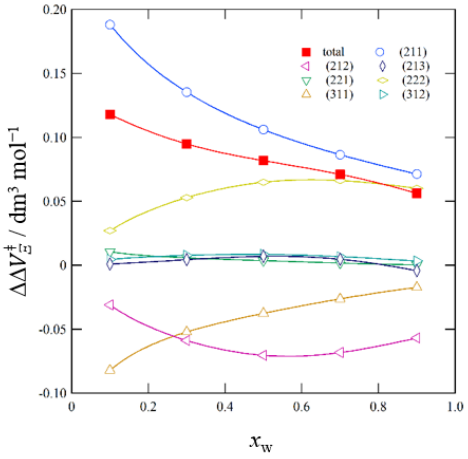

(b) 800 ºC, ρ = 1.0 M

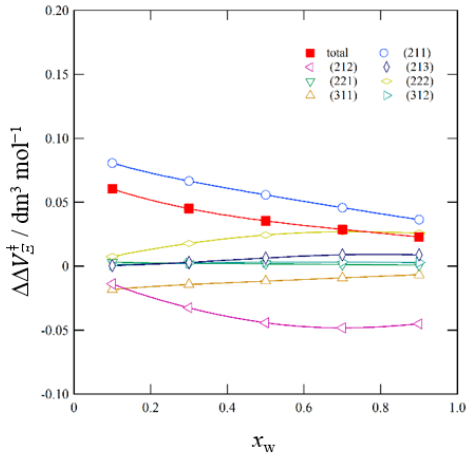

(c) 800 ºC, ρ = 2.0 M

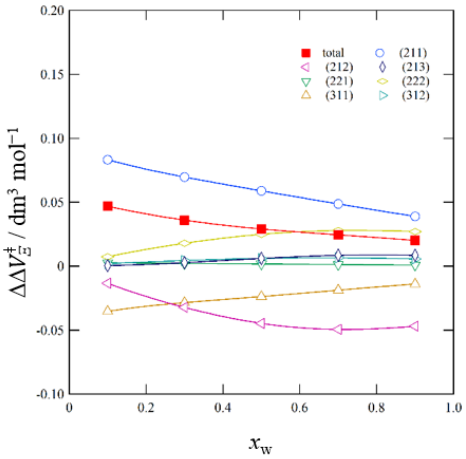

Fig. S7. Total and component differences between the activation volumes $\Delta\Delta V_{\Xi}^{\ddagger}$ and $\Delta\Delta V_{\Xi,klm}^{\ddagger}$ of water and cyclohexane (a) at 400 °C at 2.0 M, (b) water at 800 °C at 1.0 M, and (c) water at 800 °C at 2.0 M. The three-digit number for each plot indicates the subscript *klm* of $\Delta\Delta V_{\Xi,klm}^{\ddagger}$.

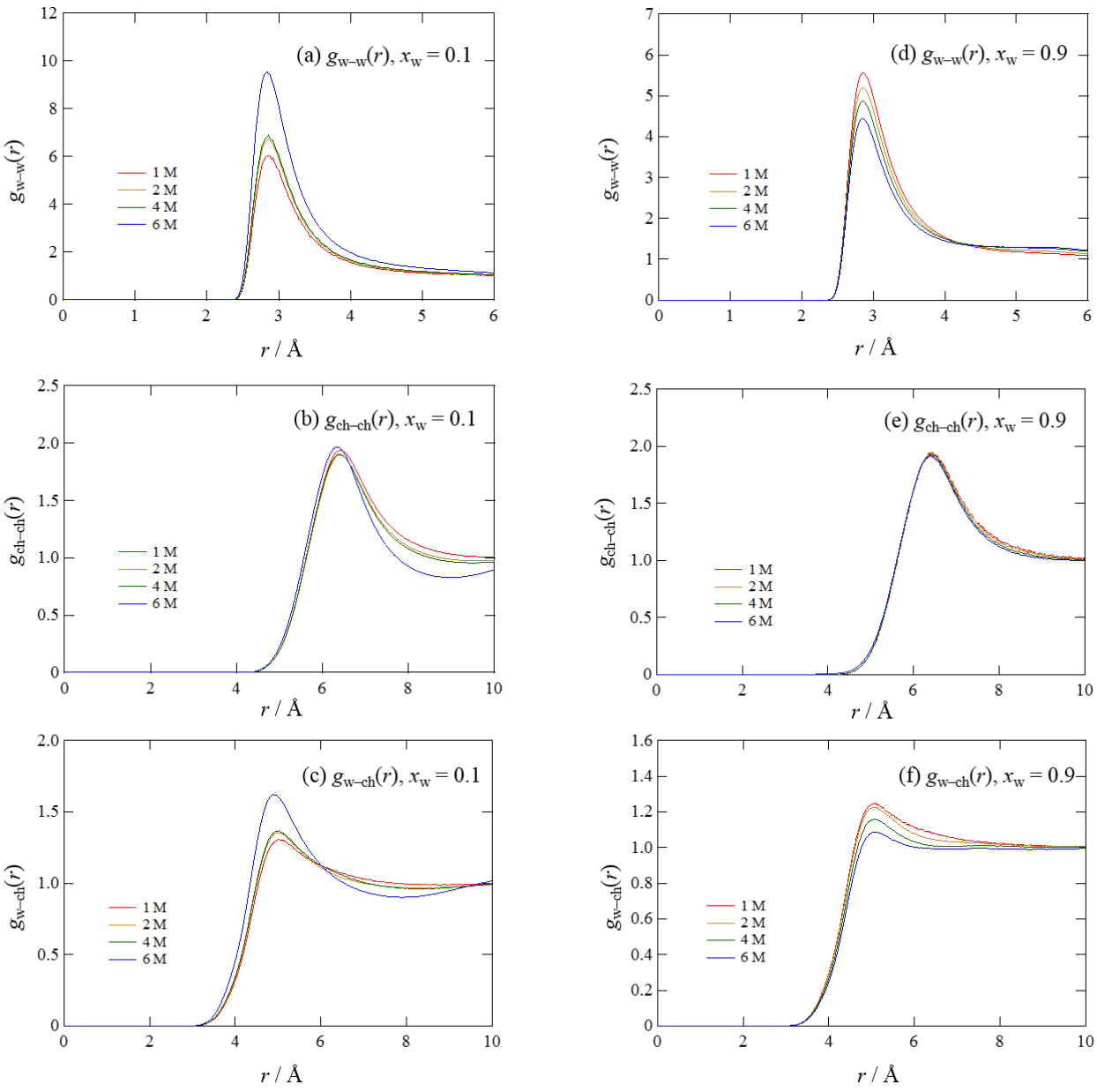

Fig. S8. Radial distribution functions (RDFs) obtained by MD simulation at 400 ºC between (a) water molecules ($g_{w\text{-}w}(r)$) at $x_w = 0.1$, (b) cyclohexane molecules ($g_{ch\text{-}ch}(r)$) at $x_w = 0.1$, and (c) water and cyclohexane ($g_{w\text{-}ch}(r)$) at $x_w = 0.1$. Panels (d), (e), and (f) show $g_{w\text{-}w}(r)$, $g_{ch\text{-}ch}(r)$, and $g_{w\text{-}ch}(r)$, respectively, at 400 ºC and $x_w = 0.9$.

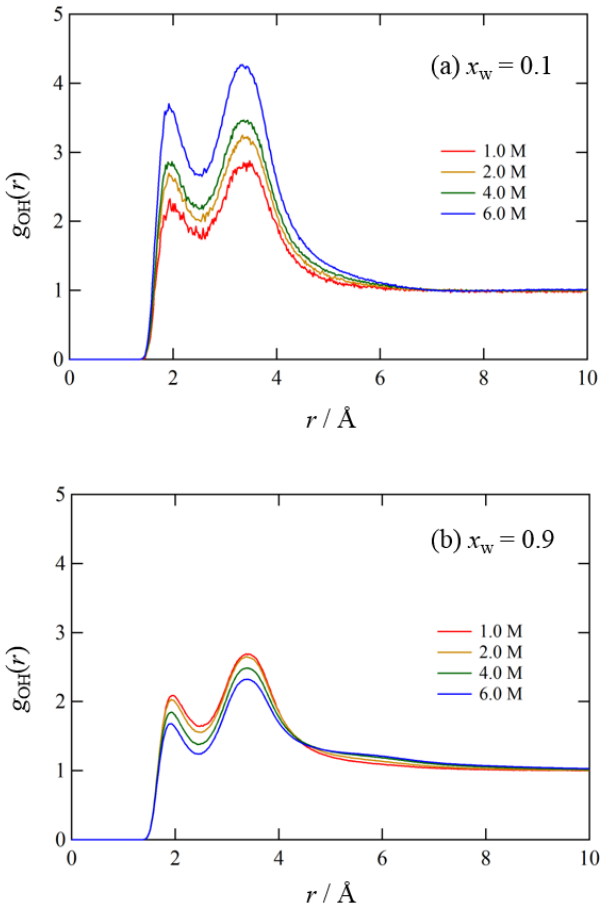

Fig. S9. Radial distribution functions (RDFs) obtained by MD simulation at 400 ºC between the oxygen and hydrogen atoms of water molecules ($g_{OH}(r)$) at (a) x_w = 0.1 and (b) x_w = 0.9.

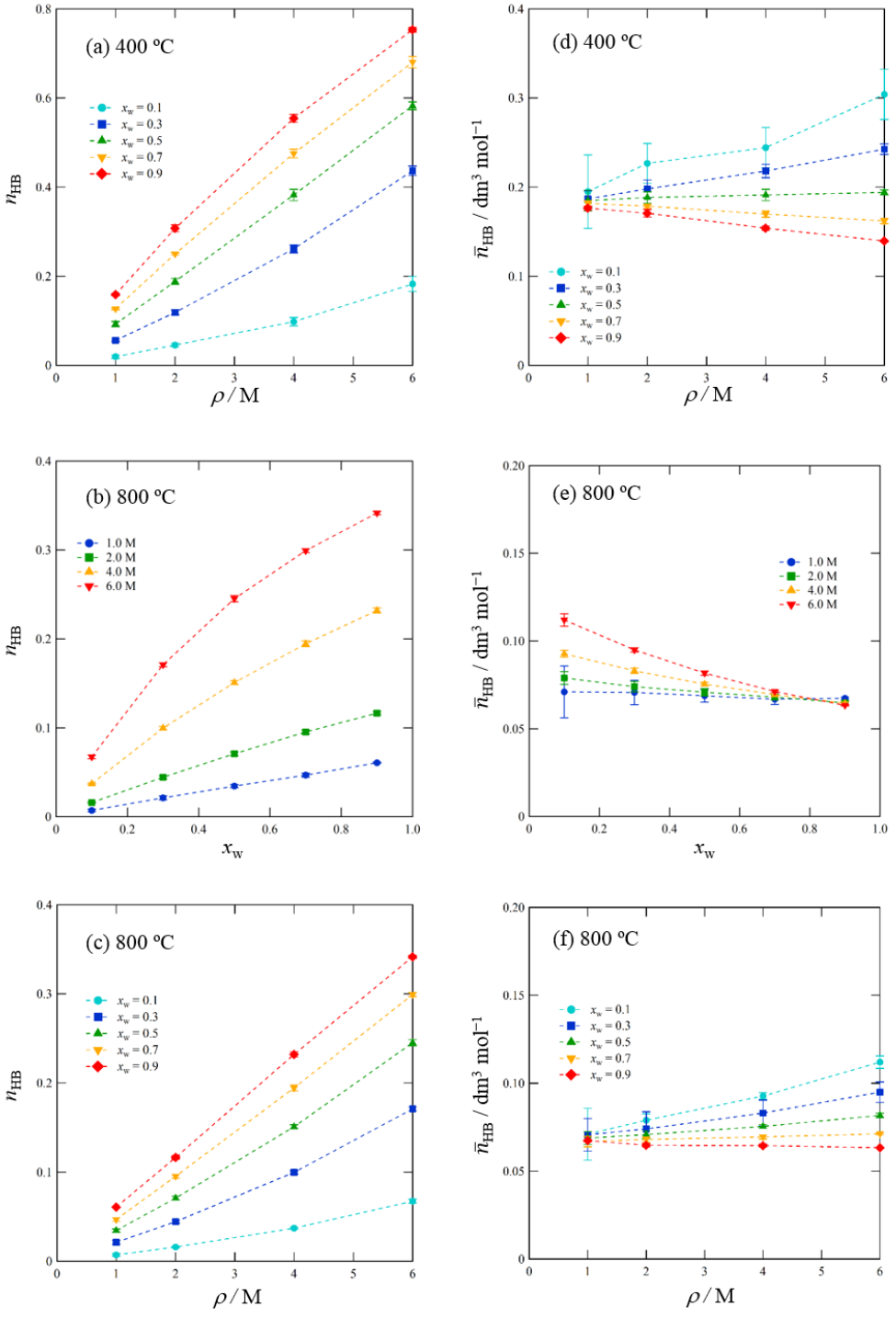

Fig. S10. Number of hydrogen bonds n_{HB} obtained by MD simulation at (a) 400 ºC plotted against ρ, (b) 800 ºC plotted against x_w, and (c) 800 ºC plotted against ρ, and the number of hydrogen bonds $\bar{n}_{HB}$ normalized to the unit molar quantity of solvent water molecules at (d) 400 ºC plotted against ρ, (e) 800 ºC plotted against x_w, and (f) 800 ºC plotted against ρ.

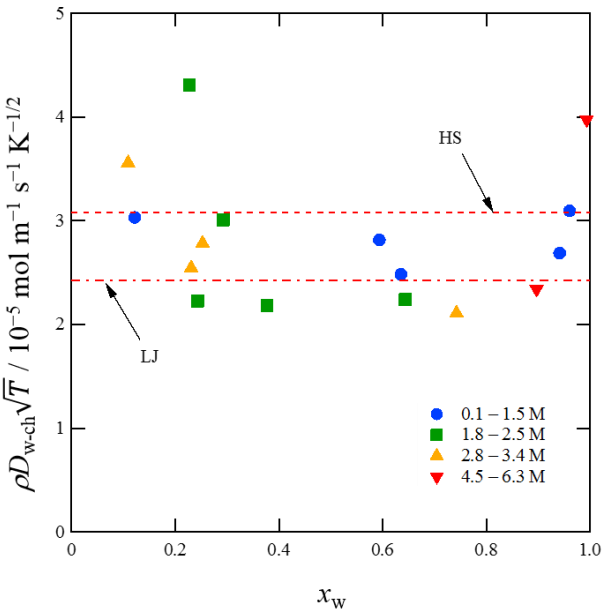

Fig. S11. Product of the density and the experimental mutual diffusion coefficient in mixtures of water and cyclohexane at 400 ºC divided by the square root of the temperature, $\rho D_{\text{w-ch}}/\sqrt{T}$, plotted against the mole fraction of water, x_{w}. The data plots are divided into groups of different density ranges and drawn with different symbols, with the density ranges in M (mol L^{-1}) indicated in the key on the figure. The horizontal lines at 3.08 and 2.43 × 10^{-5} mol m^{-1} s^{-1} K$^{-1/2}$ indicate the $\rho D_{\text{w-ch}}/\sqrt{T}$ values of the hard-sphere (HS) and Lennard–Jones (LJ) models, respectively.

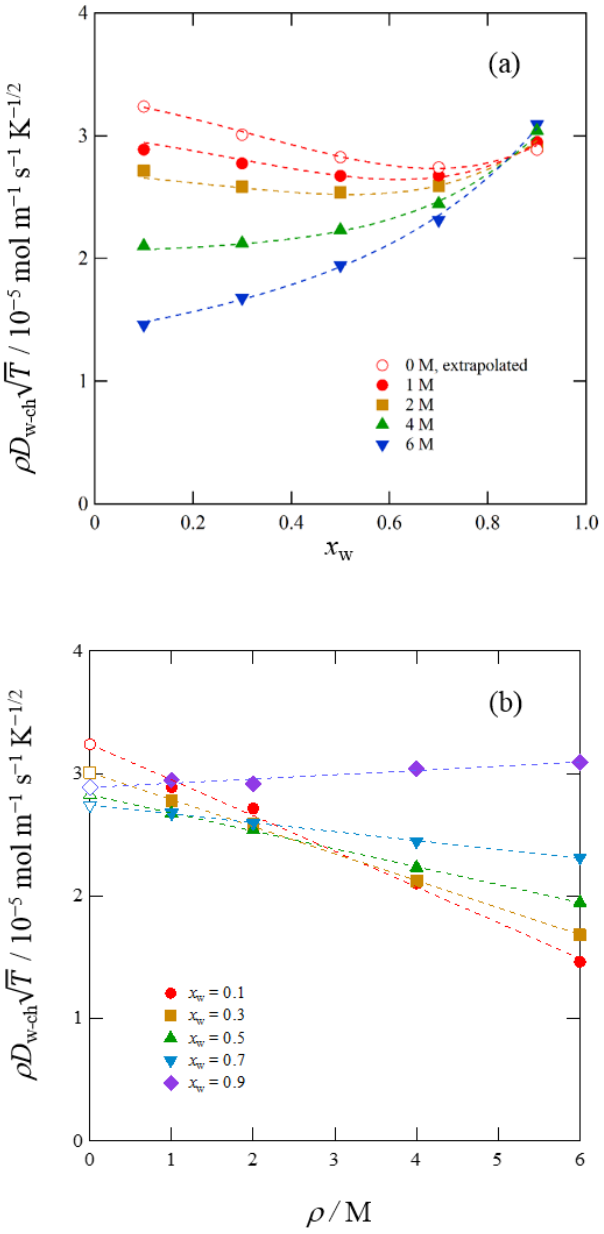

Fig. S12. Values of the product $\rho D_{\text{w-ch}}/\sqrt{T}$ obtained by MD simulation at 400 ºC plotted against (a) the mole fraction of water x_{w} and (b) the density ρ. The open red circles in (a) are those obtained from the linear extrapolation shown in (b). The dashed curves in (a) at 1.0–6.0 M are the fitted values based on Eq. (5) and that at 0 M is the calculated value based on Eq. (5) with $\rho = 1.0 \times 10^{-10}$ M.

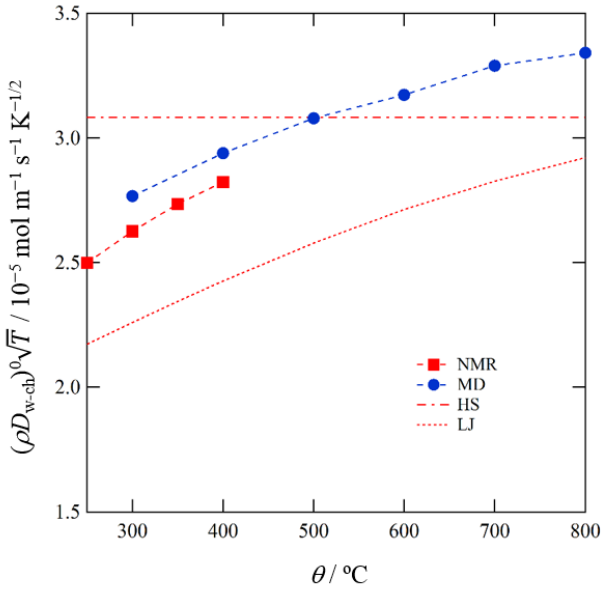

Fig. S13. Values of the product $(\rho D_{\text{w-ch}})_0/\sqrt{T}$ plotted against temperature. The $D_{\text{w-ch}}$ values for the hard-sphere (HS) and Lennard–Jones (LJ) models were calculated using Eqs. (S4) and (S5), respectively. The lines joining NMR experimental and MD simulation points are to guide the eye.

Table SI. Self-diffusion coefficients of water (D_w) and cyclohexane (D_{ch}) in binary mixtures as determined by MD simulation.

Θ / ºC	ρ / mol L^{-1}	x_w	D_w / 10^{-6} m^2 s^{-1}	D_{ch} / 10^{-6} m^2 s^{-1}
300	1.0	0.1	0.722 ± 0.003	0.223 ± 0.001
		0.3	0.780 ± 0.001	0.265 ± 0.001
		0.5	0.852 ± 0.001	0.324 ± 0.001
		0.7	0.946 ± 0.001	0.423 ± 0.001
		0.9	1.097 ± 0.001	0.620 ± 0.002
	2.0	0.1	0.338 ± 0.003	0.108 ± 0.001
		0.3	0.350 ± 0.002	0.130 ± 0.001
		0.5	0.384 ± 0.001	0.163 ± 0.001
		0.7	0.434 ± 0.001	0.216 ± 0.002
		0.9	0.509 ± 0.001	0.325 ± 0.003
	4.0	0.1	0.125 ± 0.003	0.047 ± 0.001
		0.3	0.139 ± 0.001	0.060 ± 0.001
		0.5	(0.158 ± 0.001) [a]	(0.078 ± 0.001) [a]
		0.7	(0.187 ± 0.001) [a]	(0.109 ± 0.001) [a]
		0.9	(0.234 ± 0.001) [a]	(0.180 ± 0.003) [a]
	6.0	0.1	0.057 ± 0.002	0.022 ± 0.001
		0.3	(0.068 ± 0.002) [a]	(0.033 ± 0.001) [a]
		0.5	(0.084 ± 0.001) [a]	(0.047 ± 0.001) [a]
		0.7	(0.108 ± 0.001) [a]	(0.072 ± 0.002) [a]
		0.9	(0.143 ± 0.001) [a]	(0.126 ± 0.003) [a]
400	1.0	0.1	0.804 ± 0.003	0.257 ± 0.001
		0.3	0.899 ± 0.002	0.302 ± 0.001
		0.5	1.012 ± 0.001	0.375 ± 0.001
		0.7	1.193 ± 0.001	0.480 ± 0.001
		0.9	1.408 ± 0.001	0.693 ± 0.003
	2.0	0.1	0.377 ± 0.003	0.123 ± 0.001

		0.3	0.415 ± 0.002	0.148 ± 0.001
		0.5	0.475 ± 0.001	0.183 ± 0.001
		0.7	0.558 ± 0.001	0.241 ± 0.002
		0.9	0.678 ± 0.001	0.345 ± 0.003
	4.0	0.1	0.146 ± 0.002	0.053 ± 0.001
		0.3	0.168 ± 0.002	0.067 ± 0.001
		0.5	0.202 ± 0.001	0.088 ± 0.001
		0.7	0.251 ± 0.001	0.119 ± 0.001
		0.9	0.323 ± 0.001	0.183 ± 0.003
	6.0	0.1	0.067 ± 0.002	0.026 ± 0.001
		0.3	0.088 ± 0.002	0.037 ± 0.001
		0.5	0.116 ± 0.001	0.053 ± 0.001
		0.7	0.155 ± 0.001	0.076 ± 0.002
		0.9	0.211 ± 0.001	0.125 ± 0.002
500	1.0	0.1	0.894 ± 0.003	0.290 ± 0.001
		0.3	1.024 ± 0.002	0.343 ± 0.001
		0.5	1.178 ± 0.001	0.420 ± 0.001
		0.7	1.395 ± 0.001	0.535 ± 0.002
		0.9	1.682 ± 0.001	0.733 ± 0.003
	2.0	0.1	0.409 ± 0.002	0.137 ± 0.001
		0.3	0.468 ± 0.001	0.166 ± 0.001
		0.5	0.548 ± 0.001	0.206 ± 0.001
		0.7	0.658 ± 0.001	0.268 ± 0.001
		0.9	0.826 ± 0.001	0.383 ± 0.003
	4.0	0.1	0.161 ± 0.002	0.056 ± 0.001
		0.3	0.194 ± 0.002	0.074 ± 0.001
		0.5	0.239 ± 0.001	0.097 ± 0.001
		0.7	0.305 ± 0.001	0.130 ± 0.001
		0.9	0.401 ± 0.001	0.192 ± 0.003
	6.0	0.1	0.076 ± 0.003	0.028 ± 0.001

		0.3	0.103 ± 0.002	0.041 ± 0.001
		0.5	0.138 ± 0.001	0.059 ± 0.001
		0.7	0.188 ± 0.001	0.084 ± 0.002
		0.9	0.263 ± 0.001	0.133 ± 0.002
600	1.0	0.1	0.988 ± 0.002	0.317 ± 0.001
		0.3	1.133 ± 0.002	0.375 ± 0.001
		0.5	1.294 ± 0.001	0.455 ± 0.001
		0.7	1.560 ± 0.001	0.579 ± 0.002
		0.9	1.955 ± 0.001	0.812 ± 0.003
	2.0	0.1	0.430 ± 0.003	0.149 ± 0.001
		0.3	0.499 ± 0.002	0.179 ± 0.001
		0.5	0.606 ± 0.001	0.222 ± 0.001
		0.7	0.749 ± 0.001	0.288 ± 0.002
		0.9	0.960 ± 0.001	0.400 ± 0.003
	4.0	0.1	0.176 ± 0.003	0.063 ± 0.001
		0.3	0.215 ± 0.002	0.081 ± 0.001
		0.5	0.269 ± 0.001	0.105 ± 0.001
		0.7	0.344 ± 0.001	0.139 ± 0.002
		0.9	0.472 ± 0.001	0.204 ± 0.003
	6.0	0.1	0.085 ± 0.003	0.031 ± 0.001
		0.3	0.114 ± 0.002	0.045 ± 0.001
		0.5	0.155 ± 0.001	0.063 ± 0.001
		0.7	0.215 ± 0.001	0.089 ± 0.001
		0.9	0.307 ± 0.001	0.137 ± 0.002
700	1.0	0.1	1.090 ± 0.002	0.340 ± 0.001
		0.3	1.218 ± 0.001	0.401 ± 0.001
		0.5	1.424 ± 0.001	0.488 ± 0.001
		0.7	1.731 ± 0.001	0.630 ± 0.002
		0.9	2.206 ± 0.001	0.865 ± 0.002
	2.0	0.1	0.471 ± 0.002	0.161 ± 0.001

		0.3	0.556 ± 0.002	0.193 ± 0.001
		0.5	0.668 ± 0.001	0.241 ± 0.001
		0.7	0.842 ± 0.001	0.310 ± 0.001
		0.9	1.084 ± 0.001	0.448 ± 0.003
	4.0	0.1	0.187 ± 0.003	0.067 ± 0.001
		0.3	0.230 ± 0.002	0.087 ± 0.001
		0.5	0.296 ± 0.001	0.111 ± 0.001
		0.7	0.384 ± 0.001	0.150 ± 0.001
		0.9	0.530 ± 0.001	0.219 ± 0.003
	6.0	0.1	0.092 ± 0.003	0.034 ± 0.001
		0.3	0.127 ± 0.001	0.048 ± 0.001
		0.5	0.173 ± 0.001	0.069 ± 0.001
		0.7	0.240 ± 0.001	0.096 ± 0.002
		0.9	0.346 ± 0.001	0.147 ± 0.003
800	1.0	0.1	1.108 ± 0.003	0.363 ± 0.001
		0.3	1.291 ± 0.001	0.430 ± 0.001
		0.5	1.539 ± 0.001	0.534 ± 0.001
		0.7	1.903 ± 0.001	0.675 ± 0.002
		0.9	2.449 ± 0.001	0.933 ± 0.003
	2.0	0.1	0.496 ± 0.002	0.171 ± 0.001
		0.3	0.608 ± 0.002	0.203 ± 0.001
		0.5	0.732 ± 0.001	0.259 ± 0.001
		0.7	0.910 ± 0.001	0.331 ± 0.002
		0.9	1.199 ± 0.001	0.458 ± 0.003
	4.0	0.1	0.194 ± 0.002	0.072 ± 0.001
		0.3	0.254 ± 0.001	0.092 ± 0.001
		0.5	0.324 ± 0.001	0.118 ± 0.001
		0.7	0.423 ± 0.001	0.157 ± 0.002
		0.9	0.588 ± 0.001	0.231 ± 0.002
	6.0	0.1	0.098 ± 0.003	0.036 ± 0.001

0.3	0.136 ± 0.002	0.052 ± 0.001
0.5	0.188 ± 0.001	0.072 ± 0.001
0.7	0.263 ± 0.001	0.100 ± 0.001
0.9	0.384 ± 0.001	0.157 ± 0.003

[a]The values in parentheses are omitted from the analysis of the correlation function and the activation energy.

Table SII. Values of the fitted parameters of Eq. (5) and the uncertainties in the experimental NMR self-diffusion coefficients.

Coefficient	Water		Cyclohexane	
	Value	Uncertainty (±)	Value	Uncertainty (±)
a_{111}	34.98098	2.57435	11.27647	1.551257
a_{112}	69.46678	19.00559	20.65871	11.45243
a_{113}	−79.4413	43.8826	−18.7262	26.44287
a_{114}	105.5768	29.21202	22.22026	17.60265
a_{121}	−1.262	1.926088	−1.76531	1.160627
a_{122}	−35.1822	14.79844	−1.89432	8.917277
a_{123}	48.48148	34.55299	−7.93901	20.82101
a_{124}	−58.724	23.06566	9.2907	13.89896
a_{211}	−3.27798	0.627301	−0.26813	0.378
a_{212}	−0.52419	1.307907	−1.52678	0.788121
a_{213}	2.857755	0.639282	1.363493	0.38522
a_{221}	0.152955	0.322781	0.08163	0.194502
a_{222}	−0.56115	0.605191	0.604504	0.364677
a_{311}	−0.0168	0.061952	−0.09498	0.037331
a_{312}	0.166899	0.109838	0.104184	0.066186

Table SIII. Deviations of the experimental NMR self-diffusion coefficients for water ($D_{w,NMR}$) and cyclohexane ($D_{ch,NMR}$) from the fitted values of the MD simulation ($D_{w,fit,MD}$ and $D_{ch,fit,MD}$) and the fitted values adjusted to the experimental NMR values ($D_{w,fit,NMR}$ and $D_{ch,fit,NMR}$).

Θ / °C	ρ / mol L^{-1}	x_w	$D_{w,NMR}$ / 10^{-6} m^2 s^{-1}	$D_{ch,NMR}$ / 10^{-6} m^2 s^{-1}	$\frac{D_{w,NMR}-D_{w,fit,MD}}{D_{w,fit,MD}}$	$\frac{D_{ch,NMR}-D_{ch,fit,MD}}{D_{ch,fit,MD}}$	$\frac{D_{w,NMR}-D_{w,fit,NMR}}{D_{w,fit,NMR}}$	$\frac{D_{ch,NMR}-D_{ch,fit,NMR}}{D_{ch,fit,NMR}}$
250	0.97	0.942	1.186	0.560	0.288	−0.152	0.223	−0.101
	1.05	0.594	0.864	0.318	0.155	0.001	0.097	0.061
300	0.62	0.635	1.479	0.529	−0.020	−0.143	−0.069	−0.092
	0.97	0.942	1.335	0.603	0.180	−0.138	0.120	−0.087
	1.05	0.594	0.951	0.357	0.120	0.032	0.063	0.094
	1.39	0.960	0.931	0.474	0.183	−0.075	0.123	−0.020
	1.49	0.122	0.483	0.168	0.031	0.103	−0.021	0.169
	1.88	0.377	0.343	0.124	−0.128	−0.171	−0.173	−0.121
	2.38	0.293	0.352	0.125	0.238	0.159	0.175	0.228
	2.41	0.243	0.253	0.089	−0.071	−0.12	−0.118	−0.067
	2.42	0.643	0.324	0.132	−0.055	−0.182	−0.103	−0.133
	3.07	0.252	0.238	0.085	0.194	0.093	0.134	0.158
	3.13	0.231	0.208	0.075	0.082	0.008	0.027	0.068
350	0.62	0.635	1.629	0.576	−0.031	−0.131	−0.08	−0.079
	0.97	0.942	1.509	0.650	0.137	−0.119	0.079	−0.066
	1.05	0.594	1.069	0.404	0.132	0.088	0.074	0.154

	1.39	0.960	1.051	0.517	0.132	−0.039	0.075	0.019
	1.88	0.377	0.366	0.135	−0.151	−0.159	−0.194	−0.108
	2.42	0.643	0.367	0.145	−0.049	−0.156	−0.097	−0.105
	3.13	0.231	0.225	0.084	0.077	0.050	0.022	0.113
	3.34	0.742	0.258	0.115	−0.118	−0.222	−0.163	−0.175
	4.52	0.897	0.227	0.117	−0.088	−0.24	−0.135	−0.195
400	0.62	0.635	1.771	0.619	−0.039	−0.125	−0.088	−0.072
	0.97	0.942	1.667	0.660	0.105	−0.147	0.049	−0.096
	1.05	0.594	1.123	0.408	0.087	0.031	0.032	0.093
	1.39	0.960	1.175	0.552	0.11	−0.021	0.053	0.038
	1.49	0.122	0.574	0.197	0.084	0.136	0.029	0.204
	1.88	0.377	0.397	0.143	−0.147	−0.167	−0.19	−0.117
	2.38	0.293	0.404	0.146	0.212	0.187	0.15	0.259
	2.41	0.243	0.283	0.103	−0.106	−0.111	−0.152	−0.057
	2.42	0.643	0.389	0.157	−0.089	−0.134	−0.135	−0.082
	3.07	0.252	0.280	0.100	0.203	0.132	0.142	0.200
	3.13	0.231	0.248	0.089	0.103	0.051	0.047	0.114
	3.34	0.742	0.287	0.121	−0.123	−0.225	−0.168	−0.178
	4.52	0.897	0.254	0.121	−0.108	−0.245	−0.153	−0.200
	6.35	0.994	0.324	0.162	0.394	0.110	0.323	0.177

Table SIV. Values of the fitted parameters of Eq. (5) and the uncertainties in the experimental NMR values of the self-diffusion coefficients.

Coefficient	Water		Cyclohexane	
	Value	Uncertainty (±)	Value	Uncertainty (±)
a_{111}	36.84677	2.711658	10.63656	1.463228
a_{112}	73.17193	20.01929	19.48639	10.80254
a_{113}	−83.6785	46.22317	−17.6635	24.94232
a_{114}	111.2079	30.77011	20.95932	16.60375
a_{121}	−1.32932	2.02882	−1.66514	1.094764
a_{122}	−37.0587	15.58775	−1.78683	8.411248
a_{123}	51.06735	36.39594	−7.48849	19.63948
a_{124}	−61.8562	24.29592	8.76348	13.11023
a_{211}	−3.45282	0.660759	−0.25291	0.35655
a_{212}	−0.55215	1.377667	−1.44014	0.743398
a_{213}	3.010179	0.67338	1.286119	0.36336
a_{221}	0.161113	0.339997	0.076997	0.183465
a_{222}	−0.59108	0.63747	0.5702	0.343983
a_{311}	−0.0177	0.065257	−0.08959	0.035213
a_{312}	0.175801	0.115697	0.098272	0.062431

Table SV. Effect of the deletion or addition of a term to Eq. (5) on the RMSD between the fitted curve and the MD simulation values of the self-diffusion coefficients.

Change	Term to change[a]	RMSD (%), water	RMSD (%), cyclohexane
Eq. (5)	—	1.18	1.35
Delete	124	1.29	1.36
Delete	213	1.58	1.81
Delete	222	1.15	1.50
Delete	312	1.28	1.51
Add	115	1.25	1.38
Add	131	1.23	1.54
Add	214	1.16	1.26
Add	223	1.12	1.33
Add	313	1.17	1.35
Add	321	1.20	1.30
Add	411	1.17	1.35

[a]Each term to add or delete is indicated by the subscript *klm* of the coefficient a_{klm}.

REFERENCES

[1] K. Yoshida, N. Matubayasi, and M. Nakahara, J. Chem. Phys. **129**, 214501 (2008).

[2] K. Yoshida, N. Matubayasi, and M. Nakahara, J. Chem. Phys. **125**, 074307 (2006).

[3] J. O. Hirschfelder, C. F. Curtiss, and R. B. Bird, *Molecular Theory of Gases and Liquids* (Wiley, New York, 1954),

[4] H. J. V. Tyrrell, and K. Harris, *Diffusion in Liquids* (Butterworth-Heinemann, Oxford, 1984),

[5] D. W. McCall, and D. C. Douglass, J. Phys. Chem. **71**, 987 (1967).

[6] K. Yoshida, N. Matubayasi, and M. Nakahara, J. Mol. Liq. **147**, 96 (2009).